

# Curvature induced potential on the surface of revolution and energy shift on the surface of truncated cone

Long Du<sup>1</sup> · Yong-Long Wang<sup>2,3,a</sup> · Guang-Zhen Kang<sup>2</sup> · Xiao-Jun Liu<sup>1,b</sup> · Hong-Shi Zong<sup>2,4,5,c</sup>

Received: date / Accepted: date

**Abstract** We derive the curvature induced quantum-mechanical potential of a neutral spinless particle constrained to move on a surface of revolution. Using the thin-layer quantization scheme, we decompose the tangent component of the Schrödinger equation from the transverse component. The tangent Schrödinger equation is separated into angular and axial direction in cylindrical coordinate. The exactly solvable model with the shape of truncated cone is investigated and its geometrical induced states are given analytically. With hard wall boundary condition, we find that energy levels and energy differences decrease monotonically with raising the height and generatrix slope of the geome-

try. Moreover, particles possessing higher kinetic energy tends to occupy the place with greater curvature. These results do good favor to concerned nano-structure experiment.

**Keywords** curvature induced potential, revolution, thin-layer quantization and energy shift

**PACS** 68.65.-k , 03.65.Ge , 02.40.-k

## 1 Introduction

Studying the quantum dynamics of a particle constrained to move on a 2D curved surface is a traditional subject with controversy for decades [1, 2, 3, 4, 5]. It is another important application of Riemann geometry in modern physics besides the Einstein's general relativity [6, 7]. Geometrical effects in quantum system often come into play by the internal metric of the constraint manifold when surface curvatures become comparable to the de Broglie wave length [8].

With the rapid development of nano-structure and quantum wave guides [9, 10, 11], many questions concerned with curved surface in quantum mechanics have emerged [12]. The geometrical effects were observed experimentally in some man-made nano-structures [6, 8]. At the same time, a great deal of theoretical work with various of novel geometries came out [13, 14, 15, 16]. Moreover, general theories of many fermions embedded in 2D subspace are given by Mark Burgess, Bjørn Jensen and Shigeki Matsutani [17, 18]. Giulio Ferrari and Giampaolo Cuoghi rigorously developed Schrödinger equation in general form that is valid for any 2D curved structure with electromagnetic field [19]. Recently, we studied the Pauli equation for one charged spin particle moving on a curved surface in an electromagnetic field [20].

<sup>1</sup> Key Laboratory of Modern Acoustics, MOE, Institute of Acoustics, and Department of Physics, Nanjing University, Nanjing 210093, People's Republic Of China

<sup>2</sup> Department of Physics, Nanjing University, Nanjing 210093, People's Republic Of China

<sup>3</sup> Department of Physics, School of Science, Linyi University, Linyi 276005, People's Republic Of China

<sup>4</sup> Joint Center for Particle, Nuclear Physics and Cosmology, Nanjing 210093, People's Republic Of China

<sup>5</sup> State Key Laboratory of Theoretical Physics, Institute of Theoretical Physics, CAS, Beijing 100190, People's Republic Of China

<sup>a</sup> E-mail: wylong322@163.com

<sup>b</sup> E-mail: liuxiaojun@nju.edu.cn

<sup>c</sup> E-mail: zonghs@nju.edu.cn

Nano-structure with the shape of revolution is an important artificial quantum device. Geometrical actions are investigated on some special surfaces of revolution [16, 21, 22, 23]. In this paper we firstly pay attention to the quantum dynamics of a non-relativistic neutral spinless particle on an arbitrary revolution surface and provide the general form of separable Schrödinger equation. After that, curvature induced quantum states on the surface of truncated cone are obtained analytically which provide an ideal evidence for testifying the correction and the range of application of thin-layer quantization method. Moreover, nano-structure, such as quantum dot, conjunction between nano tubes with different radius and so on, usually appears as this form. This paper is organized as follows: In Sec. 2, a general form of Schrödinger equation on revolution surface with function of generatrix,  $f(z)$ , is derived in cylindrical coordinate. The partial differential equation is separated into three independent ordinary differential equations. We apply the general results to the surface of truncated cone in Sec. 3. With hard wall boundary condition, bound states are solved analytically and the corresponding energy levels are obtained. We analyse the relation between energy shift and shape of the surface. In Sec. 4, conclusions are given.

## 2 Schrödinger equation on an arbitrary revolution surface

For the sake of convenience, the surface  $S$  is parameterized as  $\mathbf{r} = \mathbf{r}(q^1, q^2)$ , which is depicted by solid red boundary in Fig. 1(a). Two auxiliary surfaces  $S', S''$ , that are located on each side of the surface  $S$  and are locally parallel to  $S$ , enclose a subspace embedded in a three-dimensional (3D) Euclidean space. An arbitrary point  $P'$  in the subspace is

$$\mathbf{R}(q^1, q^2, q^3) = \mathbf{r}(q^1, q^2) + q^3 \mathbf{n}(q^1, q^2), \quad (1)$$

where  $\mathbf{n}(q^1, q^2)$  is the normal basis vector depending only on two curvilinear coordinates  $q^1$  and  $q^2$ . In what follows, superscripts and subscripts of the lower-case Latin letters stand for the 3D indices and assume the values 1, 2, 3. Meanwhile, superscripts and subscripts of the lower-case Greek letters denote spatial indices in curved line on surface and take the values 1, 2. Spatial covariant and contravariant derivatives are defined as  $\partial_i = \frac{\partial}{\partial q^i}$  and  $\partial^i = \frac{\partial}{\partial q_i}$  respectively. Einstein summation convention is adopted throughout. We consider an electrically neutral particle constrained on  $S$ , the Schrödinger equation reads

$$i\hbar \frac{\partial}{\partial t} \psi(\mathbf{x}, t) = \left( -\frac{\hbar^2 \nabla^2}{2m} + V_\lambda(q^3) \right) \psi(\mathbf{x}, t), \quad (2)$$

where  $\lambda$  is a parameter which measures the strength of the confinement. It satisfies the expression as follows

$$\lim_{\lambda \rightarrow \infty} V_\lambda(q^3) = \begin{cases} \infty, & q^3 = 0 \\ 0, & q^3 \neq 0 \end{cases}. \quad (3)$$

By rewriting Schrödinger equation (2) in the curvilinear coordinates  $\mathbf{q} : (q^1, q^2, q^3)$  we obtain

$$i\hbar \partial_t \psi(\mathbf{q}, t) = \frac{-\hbar^2}{2m} \sqrt{G}^{-1} \partial_i \left( \sqrt{G} G^{ij} \partial_j \psi(\mathbf{q}, t) \right) + V_\lambda(q^3) \psi(\mathbf{q}, t), \quad (4)$$

where  $G^{ij}$  is the contravariant component of 3D metric  $G_{ij}$ , which is defined as

$$G_{ij} = \partial_i \mathbf{R} \cdot \partial_j \mathbf{R}, \quad (5)$$

and  $G = \det(G_{ij})$ . From Eq. (1), the relations between  $G_{ij}$  and 2D reduced metric  $g_{\sigma\beta}$ , which is defined as  $g_{\sigma\beta} = \partial_\sigma \mathbf{r} \cdot \partial_\beta \mathbf{r}$ , on  $S$  reads

$$\begin{cases} G_{\sigma\beta} = g_{\sigma\beta} + [\alpha g + (\alpha g)^T]_{\sigma\beta} q^3 + (\alpha g \alpha^T)_{\sigma\beta} (q^3)^2, \\ G_{\sigma 3} = G_{3\sigma} = 0, \quad G_{33} = 1, \end{cases} \quad (6)$$

where  $(\alpha g)_{\sigma\beta} = \alpha_\sigma^\gamma g_{\gamma\beta}$  with  $\alpha_\sigma^\gamma$  denotes the Weingarten curvatures which yields the Gauss-Weingarten equation  $S$  [24, 25]

$$\begin{cases} \partial_\beta \partial_\sigma \mathbf{r} = \Gamma_{\sigma\beta}^\gamma \partial_\gamma \mathbf{r} + h_{\sigma\beta} \mathbf{n}, \\ \partial_\sigma \mathbf{n} = \alpha_\sigma^\beta g_{\beta\gamma} \partial_\gamma \mathbf{r} - h_{\sigma\gamma} g^{\gamma\beta} \partial_\beta \mathbf{r}, \end{cases} \quad (7)$$

where matrix  $(g^{\gamma\beta})$  indicates the reciprocal of  $(g_{\gamma\beta})$  and  $h_{\sigma\gamma}$  is the second fundamental of surface  $S$ . From Eq. (7),  $\alpha_\sigma^\beta = -h_{\sigma\gamma} g^{\gamma\beta} = \partial_\sigma \mathbf{n} \cdot \partial_\gamma \mathbf{r} g^{\gamma\beta}$ .

Let  $g = \det(g_{\sigma\beta})$ , from Eqs. (5) and (7), the relation between  $G$  and  $g$  satisfies the following expression:

$$G = \xi^2 g, \quad (8)$$

where  $\xi = 1 + \text{tr}(\alpha) q^3 + \det(\alpha) (q^3)^2$ . After introducing a new wave function  $\chi(\mathbf{q}, t) = \chi_N(q^3, t) \chi_T(q^1, q^2, t)$  with the relation  $\psi(\mathbf{q}, t) = \xi(\mathbf{q})^{-1/2} \chi(\mathbf{q}, t)$ , where  $\chi_N(q^3, t)$  and  $\chi_T(q^1, q^2, t)$  represent the normal and tangent part wave function respectively. With the limit  $q^3 \rightarrow 0$ , Eq. (4) could be separated into surface and normal components as

$$\frac{-\hbar^2}{2m} \partial_3^2 \chi_N + V_\lambda(q^3) \chi_N = i\hbar \partial_t \chi_N, \quad (9)$$

$$\frac{-\hbar^2}{2m} \left[ \frac{1}{\sqrt{g}} \partial_\sigma (\sqrt{g} g^{\sigma\beta} \partial_\beta \chi_T) - \left( \frac{1}{4} (\text{tr}(\alpha_\sigma^\beta))^2 - \det(\alpha_\sigma^\beta) \right) \chi_T \right] = i\hbar \partial_t \chi_T. \quad (10)$$

Since the confinement aforementioned raises quantum excitation energies in the normal direction far beyond those in the tangential direction, Eq. (9) could be ignored [18]. Eq. (10) describes the Schrödinger equation on the surface  $S$ .  $V_g = -\frac{\hbar^2}{2m} \left( \frac{1}{4} (\text{tr}(\alpha_\sigma^\beta))^2 - \det(\alpha_\sigma^\beta) \right)$  is the well-known geometrical potential.

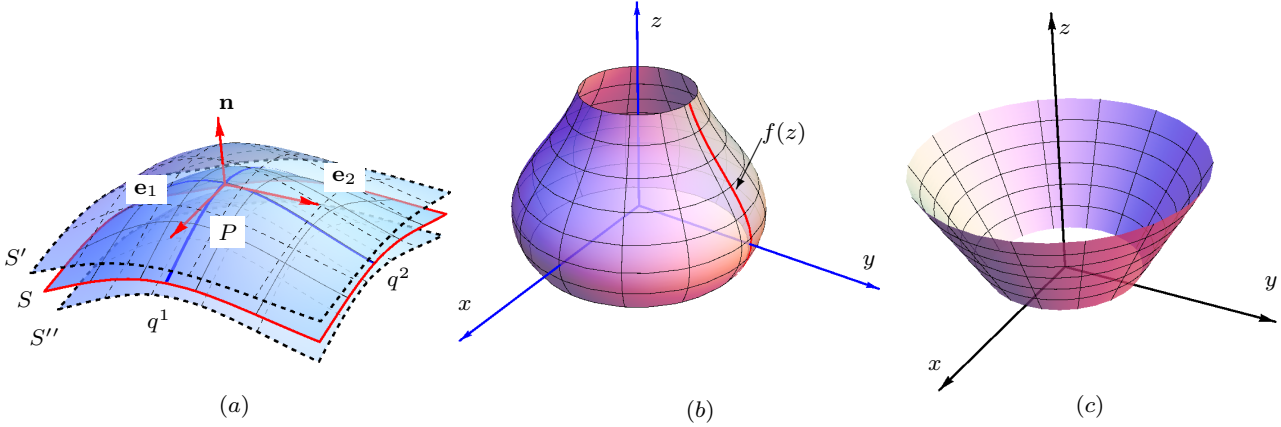


**Fig. 1** (a)(color online) Sketch shows a two-dimensional curved surface  $S$  with the curvilinear coordinates  $(q^1, q^2)$  and two auxiliary surfaces  $S', S''$ . Normal vector  $\mathbf{n}$  and  $\mathbf{e}_1, \mathbf{e}_2$  form local orthogonal frame at any point  $P$  lies on the surface  $S$ . (b) An arbitrary surface of revolution with generatrix  $f(z)$ . (c) Surface of a truncated cone.

As it shows in Fig. 1(b), a surface of revolution with generator function  $f(z)$  is axial symmetry around the  $z$  axis. Here, we suggest that  $f(z)$  is analytic and positive. In the cylindrical coordinate, a point on the surface of revolution could be parameterized as  $\mathbf{r}(\theta, z) = (f \cos \theta, f \sin \theta, z)$  and  $\partial_\theta \mathbf{r}(\theta, z) = (-f \sin \theta, f \cos \theta, 0)$ ,  $\partial_z \mathbf{r}(\theta, z) = (f_z \cos \theta, f_z \sin \theta, 1)$ , where  $f_z$  represents  $\frac{\partial}{\partial z} f$ . On the surface, the metric tensor is given by

$$g_{\sigma\beta} = \begin{pmatrix} f^2 & 0 \\ 0 & 1 + f_z^2 \end{pmatrix}. \quad (11)$$

Here,  $q^1, q^2$  are replaced by  $\theta, z$  respectively. The contravariant metric tensor of  $g^{\sigma\beta}$  is in the form

$$g^{\sigma\beta} = \begin{pmatrix} f^{-2} & 0 \\ 0 & (1 + f_z^2)^{-1} \end{pmatrix}. \quad (12)$$

The second order derivatives of vector  $\mathbf{r}(\theta, z)$  are

$$\begin{aligned} \partial_\theta^2 \mathbf{r}(\theta, z) &= (-f \cos \theta, -f \sin \theta, 0), \\ \partial_z^2 \mathbf{r}(\theta, z) &= (f_{zz} \cos \theta, f_{zz} \sin \theta, 0), \\ \partial_{\theta,z} \mathbf{r}(\theta, z) &= \partial_{z,\theta} \mathbf{r}(\theta, z) \\ &= (-f_z \sin \theta, f_z \cos \theta, 0), \end{aligned}$$

where  $f_{zz}$  indicates  $\frac{\partial^2}{\partial z^2} f(z)$ . The basis vectors lie in tangent plan with  $\mathbf{e}_1 = \partial_\theta \mathbf{r} / |\partial_\theta \mathbf{r}|$ ,  $\mathbf{e}_2 = \partial_z \mathbf{r} / |\partial_z \mathbf{r}|$  and the normal vector  $\mathbf{n}(q^1, q^2) = \mathbf{e}_1(q^1, q^2) \times \mathbf{e}_2(q^1, q^2) = \frac{1}{L(\mathbf{n})}(\cos \theta, \sin \theta, -f_z)$ , where  $L(\mathbf{n}) = \sqrt{1 + f_z^2}$ . The covariant component of second fundamental form is written as

$$h_{\sigma\beta} = \frac{1}{\sqrt{1 + f_z^2}} \begin{pmatrix} -f & 0 \\ 0 & f_{zz} \end{pmatrix} \quad (13)$$

and Weisstein tensor reads

$$\alpha_\sigma^\beta = -h_{\sigma\gamma} g^{\gamma\beta} = \frac{1}{\sqrt{1 + f_z^2}} \begin{pmatrix} \frac{1}{f} & 0 \\ 0 & -\frac{f_{zz}}{1 + f_z^2} \end{pmatrix}. \quad (14)$$

By substituting these results into Eq. (10), we obtain

$$\begin{aligned} & \frac{-\hbar^2}{2m} \left\{ \frac{1}{f^2} \partial_\theta^2 \chi_T + \frac{1}{1 + f_z^2} \partial_z^2 \chi_T \right. \\ & \left. + \frac{f_z(1 + f_z^2 - f f_{zz})}{f(1 + f_z^2)^2} \partial_z \chi_T + \frac{(1 + f_z^2 + f f_{zz})^2}{4f^2(1 + f_z^2)^3} \chi_T \right\} \\ & = i\hbar \partial_t \chi_T. \end{aligned} \quad (15)$$

By setting  $\chi_T(\theta, z, t) = \phi(\theta, z) \exp(-i\hbar\omega t)$  from Eq. (15), we obtain

$$\begin{aligned} & \frac{-\hbar^2}{2m} \left\{ f^{-2} \partial_\theta^2 \phi + \frac{1}{1 + f_z^2} \partial_z^2 \phi + \right. \\ & \left. \frac{f_z(1 + f_z^2 - f f_{zz})}{f(1 + f_z^2)^2} \partial_z \phi + \frac{(1 + f_z^2 + f f_{zz})^2}{4f^2(1 + f_z^2)^3} \phi \right. \\ & \left. + 2m\omega \phi \right\} \exp(-i\hbar\omega t) = 0. \end{aligned} \quad (16)$$

Secondly, by defining  $\phi(\theta, z) = \Theta(\theta)Z(z)$  Eq. (16) is separated into two equations following

$$\partial_\theta^2 \Theta + \eta \Theta = 0 \quad (17)$$

$$\begin{aligned} & \partial_z^2 Z + \frac{f_z(1 + f_z^2 - f f_{zz})}{f(1 + f_z^2)} \partial_z Z + \\ & \left[ \frac{(1 + f_z^2 + f f_{zz})^2}{4f^2(1 + f_z^2)^2} + 2m\omega(1 + f_z^2) \right. \\ & \left. - \frac{1 + f_z^2}{f^2} \eta \right] Z = 0, \end{aligned} \quad (18)$$

where  $\eta$  is a constant that is independent of  $\theta$  or  $z$ . Eqs. (17) and (18) give the general form of the Schrödinger equation on the revolution surface.

### 3 Curvature induced states on the surface of truncated cone

We'd like to apply the general form of Schrödinger equation to study curvature induced potential on the model with the shape of truncated cone. The surface of truncated cone is defined by revolving a line segment around a coplanar axis (Fig. 1(c)) which could be parameterized as  $f(z) = \rho + \lambda z$ , where  $\rho$  is the radius of the circle at the bottom and  $\lambda$  indicates slope of the angle between the line segment and the  $z$  axis. For definiteness and without loss of generality, we suggest  $0 < \lambda < 1$ . Thus,  $f_z = \lambda, f_{zz} = 0$ . From Eq. (18), we obtain

$$\partial_z^2 Z + \frac{\lambda}{\rho + \lambda z} \partial_z Z + \left[ \frac{1}{(\rho + \lambda z)^2} \left( \frac{1}{4} - \eta(1 + \lambda^2) \right) + 2m\omega(1 + \lambda^2) \right] Z = 0. \quad (19)$$

With the periodical boundary condition  $\phi(\theta + 2\pi, z) = \phi(\theta, z)$  and the hard wall boundary conditions,  $\phi(\theta, 0) = \phi(\theta, z_m) = 0$ , wave functions  $\Theta(\theta)$  and  $Z(z)$  should satisfy  $\Theta(\theta + 2\pi) = \Theta(\theta)$  and  $Z(0) = Z(z_m) = 0$  respectively, where  $z_m$  represents the maximum of  $z$ . The angular part solution of Eq. (17) could be written as

$$\Theta(\theta) = C_1 e^{i\sqrt{\eta}\theta} + C_2 e^{-i\sqrt{\eta}\theta}, \quad (20)$$

where  $C_1, C_2$  are complex coefficients that is independent of  $\theta$ .  $\sqrt{\eta}$  should be  $0, 1, 2, 3 \dots$  for meeting boundary condition of  $\theta$ .

Replacing  $\rho + \lambda z$  by  $y$ , Eq. (19) reads

$$\partial_y^2 Z + \frac{1}{y} \partial_y Z + \left[ \frac{1}{y^2} \left( \frac{1}{4\lambda^2} - \frac{\eta(1 + \lambda^2)}{\lambda^2} \right) + \frac{2m\omega(1 + \lambda^2)}{\lambda^2} \right] Z = 0, \quad (21)$$

which agrees with the form of Bessel equation with positive  $2m\omega(1 + \lambda^2)/(\lambda^2)$ . The axial direction wave function of Eq. (21) can be expressed as

$$Z(z) = S_1 J_{\delta(\eta, \lambda)} \left( \frac{\sqrt{2m\omega(1 + \lambda^2)}}{\lambda} (\rho + \lambda z) \right) + S_2 Y_{\delta(\eta, \lambda)} \left( \frac{\sqrt{2m\omega(1 + \lambda^2)}}{\lambda} (\rho + \lambda z) \right) \quad (22)$$

with  $\sqrt{\eta} = 0, 1, 2, 3 \dots$ ,

where  $\delta(\eta, \lambda) = \frac{1}{\lambda} \sqrt{\eta(1 + \lambda^2) - \frac{1}{4}}$ .  $J_\nu(x)$  is the Bessel function, and  $Y_\nu(x)$  represents the Neumann function (Bessel function of the second kind). Coefficients  $S_1, S_2$  adjust the proportion of these two kinds of Bessel function to meet the boundary condition of the  $z$  component and the ratio,  $-S_1/S_2$ , could be determined by the

following equation

$$Y_\delta \left( c \sqrt{\frac{1 + \lambda^2}{\lambda^2}} \right) J_\delta \left( c \sqrt{\frac{1 + \lambda^2}{\lambda^2}} \left( 1 + \frac{z_m}{\rho} \lambda \right) \right) - J_\delta \left( c \sqrt{\frac{1 + \lambda^2}{\lambda^2}} \right) Y_\delta \left( c \sqrt{\frac{1 + \lambda^2}{\lambda^2}} \left( 1 + \frac{z_m}{\rho} \lambda \right) \right) = 0, \quad (23)$$

where  $c = \rho \sqrt{2m\omega}$ . This is equivalent to  $Z(z = 0) = Z(z = z_m) = 0$ .  $\omega$ , denoting energy, could be identified. Wave function of  $z$  is written as

$$Z(z) = A \left\{ J_\delta \left[ c \left( 1 + \lambda \frac{z}{\rho} \right) \right] + \frac{-J_\delta(c)}{Y_\delta(c)} Y_\delta \left[ c \left( 1 + \lambda \frac{z}{\rho} \right) \right] \right\}, \quad (24)$$

where  $A$  represents a normalized coefficient.

Tab. 1 classifies different values of the height of the truncated cone with  $\eta = 0, \lambda = 1$ . With each fixed  $z_m/\rho$ , three bound states with the lowest eigenvalues of  $\rho \sqrt{2m\omega}$  and the corresponding eigenvectors are given.  $\eta = 0$  means that the wave function of  $\Theta(\theta)$  is a constant. Tab. 2 enumerates the results with  $\eta = 1, \lambda = 1.5$ . It is worth noting that all eigenvalues and eigenvectors could be exactly solved in principle. Fig. 2(a) depicts the distribution of possibility densities (PDs) along the  $z$  axis in Tab. 1 with  $z_m/\rho = 1.5$ . The blue, red and yellow line, which has one, two and three peaks respectively, denotes the normalized possibility density with respect to  $\rho \sqrt{2m\omega} = 1.451, 2.946$  and  $4.432$ . Similarly, PDs with  $z_m/\rho = 2, 4$  in Tab. 1 are illustrated in Fig. 2(b) and Fig. 2(c) respectively. PDs in Tab. 2 are shown in Fig. 3. The uneven geometrical potential on the surface tends to abstract particle, especially with higher energy, to the place with lower geometrical potential.

The energy levels of bound states depend on the geometric shape of the truncated cone which is described by  $\lambda$  and  $z_m$ . Functional dependence between the values of three lowest energy levels and slope of generatrix with different  $z_m$  in the case of  $\eta = 0$  are illustrated in Fig. 4(a). Energy levels and energy differences monotonously decrease with  $\lambda$ . Similarly, energy shifts in the case of  $\eta = 1$  are depicted in Fig. 4(b). The relation between the energy shift of the ground states and the height of the truncated cone,  $z_m$ , are shown in Fig. 5. The case of  $\eta = 0$  and  $\eta = 4$  are depicted in Fig. 5(a) and Fig. 5(b) respectively. When  $\lambda$  is fixed, increasing height will lower the ground state energy levels.

It is worth mentioning that two special truncated cones, cone and cylinder, could be included in this model by limiting parameters in Eq. (19). On the one hand, when  $\rho$  goes to zero, Eq. (19) is reduced to describe the  $z$  component wave function on the cone which is concerned with the C. Filgueiras et al.'s study [26]. With

$z_m \rho^{-1}$	$\rho \sqrt{2m\omega}$	$Z(z)$
1.5	1.451	$0.2905 \left( J_{\frac{1}{2}} \left( \frac{2.052(z+\rho)}{\rho} \right) - (0.2323 + 0.7231i) Y_{\frac{1}{2}} \left( \frac{2.052(z+\rho)}{\rho} \right) \right)$
	2.946	$0.2957 \left( J_{\frac{1}{2}} \left( \frac{4.166(z+\rho)}{\rho} \right) - (0.2243 + 1.462i) Y_{\frac{1}{2}} \left( \frac{4.166(z+\rho)}{\rho} \right) \right)$
	4.432	$0.1877 \left( J_{\frac{1}{2}} \left( \frac{6.268(z+\rho)}{\rho} \right) + (0.3795 - 0.8787i) Y_{\frac{1}{2}} \left( \frac{6.268(z+\rho)}{\rho} \right) \right)$
2	1.079	$0.445 \left( J_{\frac{1}{2}} \left( \frac{1.526(z+\rho)}{\rho} \right) - (0.4343 + 1.075i) Y_{\frac{1}{2}} \left( \frac{1.526(z+\rho)}{\rho} \right) \right)$
	2.204	$0.284 \left( J_{\frac{1}{2}} \left( \frac{3.117(z+\rho)}{\rho} \right) + (0.3612 - 0.8488i) Y_{\frac{1}{2}} \left( \frac{3.117(z+\rho)}{\rho} \right) \right)$
	3.320	$0.2491 \left( J_{\frac{1}{2}} \left( \frac{4.695(z+\rho)}{\rho} \right) - (0.4177 + 0.9706i) Y_{\frac{1}{2}} \left( \frac{4.695(z+\rho)}{\rho} \right) \right)$
4	0.5233	$0.8447 \left( J_{\frac{1}{2}} \left( \frac{0.74(z+\rho)}{\rho} \right) + (0.3293 - 1.374i) Y_{\frac{1}{2}} \left( \frac{0.74(z+\rho)}{\rho} \right) \right)$
	1.091	$0.5364 \left( J_{\frac{1}{2}} \left( \frac{1.543(z+\rho)}{\rho} \right) - (0.4333 + 1.057i) Y_{\frac{1}{2}} \left( \frac{1.543(z+\rho)}{\rho} \right) \right)$
	1.652	$0.3495 \left( J_{\frac{1}{2}} \left( \frac{2.337(z+\rho)}{\rho} \right) - (0.06785 + 0.6611i) Y_{\frac{1}{2}} \left( \frac{2.337(z+\rho)}{\rho} \right) \right)$

**Table 1** The solutions of Eq. (21) with  $\eta = 0, \lambda = 1$ . The lowest two energy levels and normalised wave functions of  $Z$  component are enumerated.

$z_m \rho^{-1}$	$\rho \sqrt{2m\omega}$	$Z(z)$
1.5	1.239	$0.5677 J_{1.155} \left( \frac{2.234z}{\rho} + 1.489 \right) + 0.5624 Y_{1.155} \left( \frac{2.234z}{\rho} + 1.489 \right)$
	2.369	$0.709 J_{1.155} \left( \frac{4.271z}{\rho} + 2.848 \right) - 1.544 Y_{1.155} \left( \frac{4.271z}{\rho} + 2.848 \right)$
	3.517	$0.2473 J_{1.155} \left( \frac{6.341z}{\rho} + 4.227 \right) + 0.04564 Y_{1.155} \left( \frac{6.341z}{\rho} + 4.227 \right)$
2	0.9478	$0.5637 J_{1.155} \left( \frac{1.709z}{\rho} + 1.139 \right) + 0.3101 Y_{1.155} \left( \frac{1.709z}{\rho} + 1.139 \right)$
	1.790	$1.742 J_{1.155} \left( \frac{3.228z}{\rho} + 2.152 \right) + 8.051 Y_{1.155} \left( \frac{3.228z}{\rho} + 2.152 \right)$
	2.648	$0.447 J_{1.155} \left( \frac{4.773z}{\rho} + 3.182 \right) - 0.4825 Y_{1.155} \left( \frac{4.773z}{\rho} + 3.182 \right)$
4	0.4990	$0.7723 J_{1.155} \left( \frac{0.8995z}{\rho} + 0.5997 \right) + 0.12 Y_{1.155} \left( \frac{0.8995z}{\rho} + 0.5997 \right)$
	0.9173	$0.6734 J_{1.155} \left( \frac{1.654z}{\rho} + 1.103 \right) + 0.3469 Y_{1.155} \left( \frac{1.654z}{\rho} + 1.103 \right)$
	1.342	$0.7921 J_{1.155} \left( \frac{2.419z}{\rho} + 1.613 \right) + 0.9661 Y_{1.155} \left( \frac{2.419z}{\rho} + 1.613 \right)$

**Table 2** The solutions of Eq. (21) with  $\eta = 1, \lambda = 1.5$ . The lowest two energy levels and normalised wave functions of  $Z$  component are enumerated.

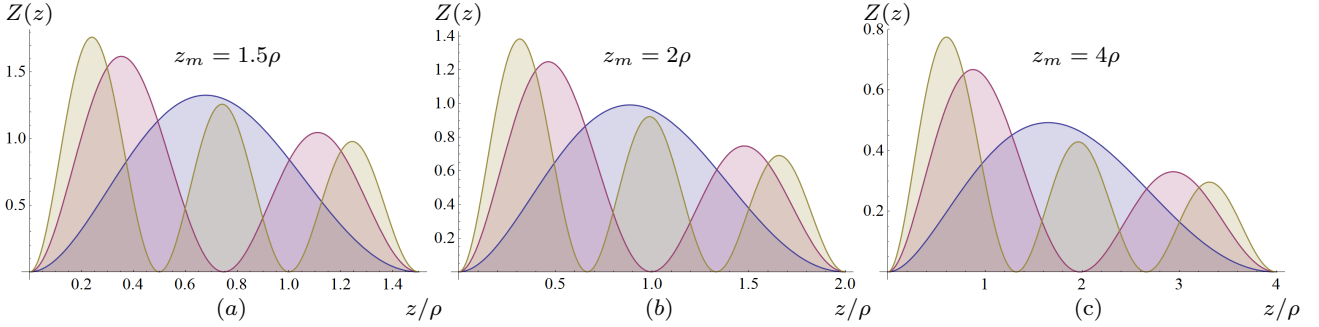


**Fig. 2** (color online) Possibility densities with  $\eta = 0, \lambda = 1$ .

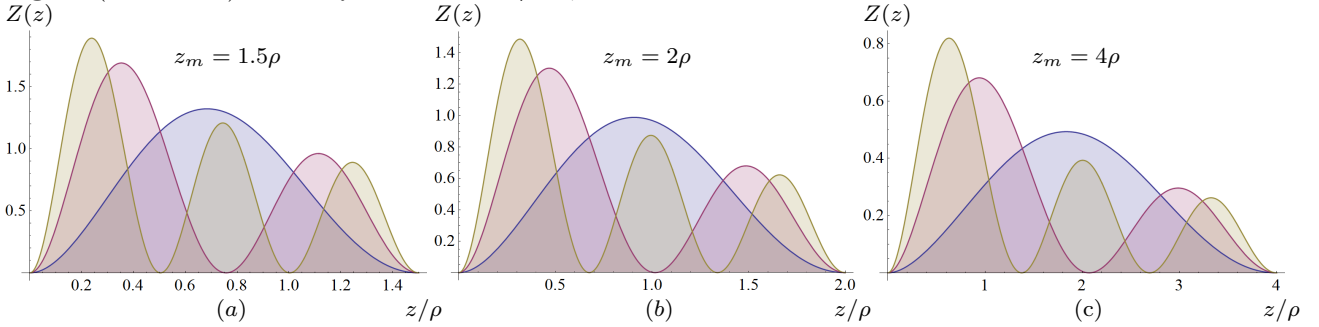


**Fig. 3** (color online) Possibility densities with  $\eta = 1, \lambda = 1.5$ .

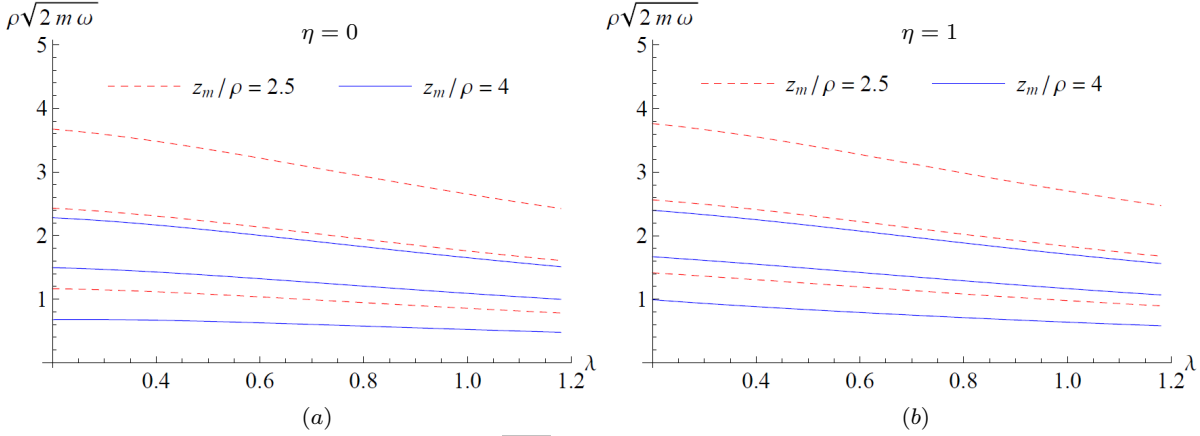


**Fig. 4** (color online) The relation between  $\rho\sqrt{2m\omega}$  and  $\lambda$ . The solid blue lines in both (a) and (b) indicate the lowest three energy levels as functions of  $\lambda$  with  $\eta = 0, 1$  respectively when  $z_m/\rho = 4$ . Similarly, the red dash lines represent the same results when  $z_m/\rho = 2.5$ .

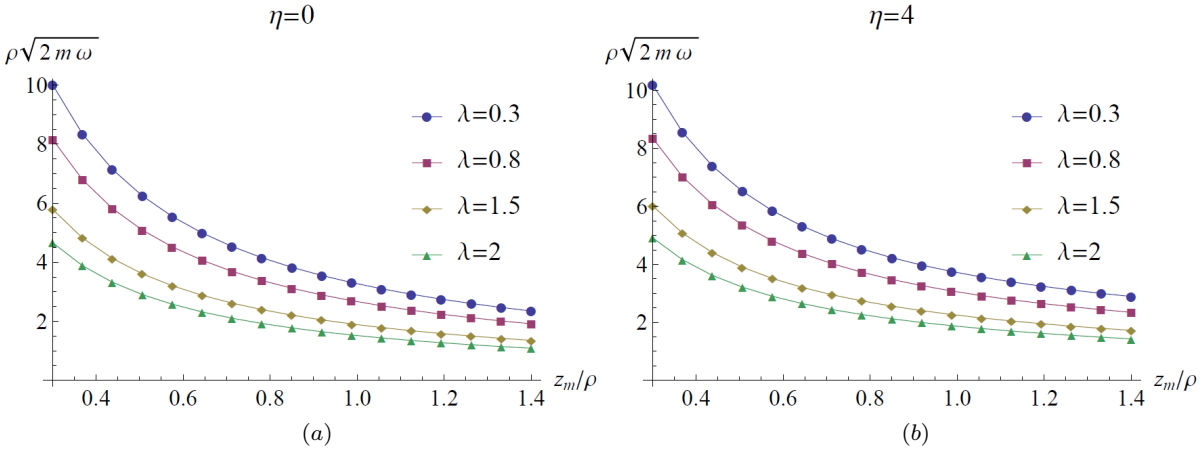


**Fig. 5** (color online) The lowest energy levels' shift  $\rho\sqrt{2m\omega}$  as a function of  $z_m/\rho$  with several values of  $\lambda$ . (a) Energy shifts in the case of  $\eta = 0$ . (b) Energy shifts in the case of  $\eta = 4$ .

the hard wall boundary condition, the Neumann function in Eq. (22) should be omitted because of its singularity at 0. On the other hand, when  $\lambda$  goes to zero Eq. (19) will be transformed to give  $z$  component wave function on the surface of cylinder.

#### 4 Conclusion

In this paper, we have studied the quantum dynamics of a neutral spinless particle confined on a surface of revolution with generatrix  $f(z)$ . The general form of the separable Schrödinger equations has been given in cylindrical coordinate. Curvature induced states with hard wall boundary condition in the  $z$  direction on the surface of truncated cone are obtained with analytic form. Graphics of possibility densities reveal that particles with higher kinetic energy tend to make itself distribute at the place with larger curvature. We have analyzed the relation between the energy shifts and the geometrical characters of this model. Solutions

of this kind of significant model of nano-structure provide useful eigenvectors for perturbation calculation of the system with geometrical potential predominant. In another word, it will be conducive to design of 2D nano-structure.

#### 5 Acknowledgement

This work is supported by the National Natural Science Foundation of China (under Grant No. 11047020, No. 11404157, No. 11274166, No. 11275097, and No. 11475085), the National Basic Research Program of China (under Grant No. 2012CB921504), the Natural Science Foundation of Shandong Province of China (under Grant No. ZR2012AM022, and No. ZR2011AM019) and the Jiangsu Planned Projects for Postdoctoral Research Funds (under Grant No. 1401113C)

## References

1. B. De Witt, Phys. Rev. **85**, 635 (1952).
2. H. Jensen, Ann. Phys. **63**, 586 (1971).
3. R. C. T. da Costa, Phys. Rev. A **23**, 1982 (1981).
4. R. C. T. da Costa, Phys. Rev. A **25**, 2893 (1982).
5. B. Jensen and R. Dandoloff, Phys. Rev. A **80**, 052109 (2009).
6. J. Onoe, T. Ito, H. Shima and etc., Euro. Phys. Lett., **98** 27001 (2012).
7. I. B. Khriplovich, General Relativity (Springer,2005).
8. A. Szameit, F. Dreisow, M. Heinrich, R. Keil, S. Nolte, A. Tunnermann, S. Longhi, Phys. Rev. Lett. **104**, 150403 (2010).
9. M. Toreblad, M. Borgh, M. Koskinen, M. Manninen, and S. M. Reimann, Phys. Rev. Lett. **93**, 090407 (2004).
10. I.Y. Popov, Phys. Lett. A **269**, 148 (2000).
11. J. Goldstone and R.L. Jaffe, Phys. Rev. B **45**, 14100 (1992).
12. M. Encinosa and L. Mott, Phys. Rev. A **68**, 014102 (2003).
13. V. Atanasov and R. Dandoloff, Phys. Lett. A **372**, 6141-6144 (2008).
14. V. Atanasov, R. Dandoloff, and A. Saxena, Phys. Rev. B **79**, 033404 (2009).
15. R. Dandoloff, A. Saxena, and B. Jensen, Phys. Rev. A **81**, 014102 (2010).
16. M. Encinosa and B. Etemadi, Phys. Rev. A **58**, 77 (1998).
17. M. Burgess and Bjørn Jensen, Phys. Rev. A **48** 1861 (1993).
18. S. Matsutani, Phys. Rev. A **47** 686 (1993).
19. G. Ferrari and G. Cuoghi, Phys. Rev. Lett. **100**, 230403 (2008).
20. Y.L. Wang, L. Du, C.T. Xu, X.J. Liu, and H.S. Zong, Phys. Rev. A **90** 042117 (2014)
21. H. Shima, H. Yoshioka, and J. Onoe, Phys. Rev. B **79**, 201401(R)(2009).
22. H. Taira and H. Shima, Surf. Scie. **601**, 22 (2007).
23. V. Atanasova, R. Dandoloff, Phys. Lett. A **371** 118123 (2007) .
24. E. Weisstein, Weingarten Equations (2008), URL <http://mathworld.wolfram.com/WeingartenEquations.html>.
25. S. S. Chern, W. H. Chen and K. S. Lam, *Lectures on differential geometry* (World Science, 1999).
26. C. Filgueiras, E. O. Silva, and F. M. Andrade, Journal of Mathematical Physics **53**, 122106 (2012)